Apoptosis is augmented in high-grade serous ovarian cancer by the combined inhibition of Bcl-2/Bcl-xL and PARP

TAKUHEI YOKOYAMA, ELISE C. KOHN, ETHAN BRILL and JUNG-MIN LEE

Women's Malignancies Branch, Center for Cancer Research, National Cancer Institute, Bethesda, MD, USA

Received November 16, 2016; Accepted January 17, 2017

DOI: 10.3892/ijo.2017.3914

Abstract. The aim of our study was to evaluate possible synergistic cytotoxic effects of the combination treatment with the BH3-mimetic ABT-263 and the PARP inhibitor BMN 673 in high-grade serous ovarian cancer (HGSOC) cells using clinically achievable concentrations of each drug. *In vitro* cytotoxic effects of ABT-263 and BMN 673 were assessed by XTT assay in three HGSOC cell lines: OVCAR3, OVCAR8, and OV90 cells. Combination index values and synergy/antagonism volumes were used to determine synergy. The drug effects on DNA damage accumulation, cell cycle progression, apoptosis induction, and expression levels of Bcl-2 family proteins were examined to dissect molecular mechanisms. The combination treatment synergistically decreased cell viability in a concentration- and time-dependent manner in all cell lines; combination index values were <0.9 and synergy/antagonism volumes were >100 after 72 h of treatment. Clinically achievable concentrations of ABT-263 2 μM and BMN 673 25 nM were used to investigate mechanisms. No increase in γ-H2AX foci formation was observed with addition of ABT-263 to BMN 673 treatment. The combination treatment increased the sub-G1 and Annexin V-positive cell populations after 48 h compared with the control and each monotherapy. It also induced greater caspase-3/7 activity and PARP cleavage. ABT-263 alone and in combination with BMN 673 induced expression levels of Bim, a pro-apoptotic protein. In conclusion, the ABT-263 and BMN 673 combination resulted in synergistic cytotoxic effects against HGSOC cells through greater induction of apoptosis. This may be a novel therapeutic strategy for HGSOC.

Correspondence to: Dr Jung-Min Lee, Women's Malignancies Branch, Center for Cancer Research, National Cancer Institute, 10 Center Drive, MSC1906, Building 10, Room 4B54, Bethesda, MD 20892-1906, USA
E-mail: leej6@mail.nih.gov

Abbreviations: HGSOC, high-grade serous ovarian cancer; PARPi, PARP inhibitor

Key words: ovarian cancer, BH3-mimetic, PARP inhibitor, apoptosis, synergy

Introduction

Ovarian cancer is the leading cause of death from gynecologic malignancies in the United States (1). Most cases of ovarian cancer present with advanced-stage disease and despite an initial high treatment response rate, the majority of patients eventually develop chemotherapy resistance (2). High-grade serous ovarian cancer (HGSOC) accounts for 70-80% of epithelial ovarian cancer cases. *BRCA* wild-type HGSOC patients in particular have a worse survival compared to both germline and somatic *BRCA* mutated HGSOC, and there remain unmet therapeutic needs for them (3,4).

PARP inhibition has demonstrated clinical activity against HGSOC, especially in deleterious germline *BRCA* mutation carriers and platinum-sensitive diseases (5). Olaparib is the first US Food and Drug Administration-approved PARP inhibitor (PARPi), licensed for use in heavily pretreated germline *BRCA* mutation-associated ovarian cancer (6). There are several other PARPi currently in the late phase clinical trial development, including niraparib, rucaparib, veliparib, and BMN 673 (talazoparib) (7). BMN 673 is a potent oral PARPi with a greater DNA-PARP trapping activity compared with other PARPi (8). Thus far, PARPi monotherapy has shown limited activity against *BRCA* wild-type HGSOC, highlighting the need for combination strategies.

PARP1, the dominant isoform responsible for the majority of PARP activity, is involved in various modes of cell death including apoptosis, parthanatos, necroptosis, and autophagy, in addition to DNA damage repair (9). PARP1 is cleaved and poly(ADP-ribosyl)ation is inhibited during apoptosis (9). PARP1 activation and accumulation of poly(ADP-ribose), by contrast, is essential for initiating or progressing the other cell death pathways (9). Thus, drugs targeting apoptotic pathways would be a suitable candidate for combination with PARPi.

Bcl-2 family proteins play a critical role in regulating the intrinsic apoptotic pathway. Major Bcl-2 family proteins include the anti-apoptotic proteins (Bcl-2, Bcl-xL, Bcl-w, and Mcl-1), pro-apoptotic effector proteins (Bax and Bak), and pro-apoptotic BH3-only proteins (Bim, Bid, Bad, Puma, and Noxa) (10). Bcl-xL is overexpressed in the majority of recurrent, chemoresistant ovarian cancer, and its expression in primary ovarian tumor is associated with a shorter disease-free interval (11,12). Preclinical studies showed inhibition of Bcl-xL increased sensitivity of ovarian cancer cells to chemotherapeutic agents (12,13). These data support

anti-apoptotic protein inhibition as a promising therapeutic direction for recurrent ovarian cancer. ABT-263 is an orally available Bad-like BH3 mimetic. ABT-263 competes with BH3-only proteins for binding to anti-apoptotic proteins, thereby preventing anti-apoptotic proteins from constraining pro-apoptotic proteins (10). ABT-263 has an inhibitory activity against Bcl-2, Bcl-xL, and Bcl-w, but not against the other anti-apoptotic protein Mcl-1 (10). This may partly explain the limited monotherapy activity of ABT-263 against solid tumors (14), although ABT-263 treatment has demonstrated favorable clinical outcome in hematological malignancies as a monotherapy (15).

We hypothesized that PARPi-induced cytotoxicity may be augmented by inhibition of anti-apoptotic proteins. Our aim was to evaluate the preclinical efficacy of the BH3-mimetic ABT-263 in combination with the PARPi BMN 673 in HGSOC cells at clinically achievable concentrations.

Materials and methods

Compounds. ABT-263 and BMN 673 were purchased from Selleck Chemicals (Houston, TX, USA). Stock solutions of ABT-263 and BMN 673 were made in DMSO at 100 mM and 20 mM, respectively. Aliquots were stored at -80˚C and diluted in culture medium at least 1:10,000 immediately before use.

Cell culture. Three *BRCA* wild-type HGSOC cell lines were used (16): OVCAR3 (purchased from ATCC, Manassas, VA, USA), OVCAR8 (obtained from the NCI-Frederick DCTD tumor/cell line repository, Frederick, MD, USA), and OV90 (generously gifted from Dr C.M. Annunziata, NCI/NIH, Bethesda, MD, USA). All cell lines were cultured in RPMI-1640 medium with L-glutamine, supplemented with 10% FBS and 1% penicillin-streptomycin under a humidified atmosphere of 5% CO_2 at 37˚C. Drug treatments were performed 24 h after initial seeding. All cell lines were tested and authenticated in March 2016 at NCI-Frederick Protein Expression Laboratory. Briefly, DNA was extracted from each cell pellet and amplified by PCR using the AmpFLSTR Identifiler PCR Amplification kit (Applied Biosystems, Foster City, CA, USA). The Identifiler kit amplifies 15 tetranucleotide repeat loci and the Amelogenin gender determination marker in a single PCR amplification. PCR-amplified fragments were analyzed on the Applied Biosystems 3130xl genetic analyzer (Applied Biosystems) in Hi-Di formamide with a size standard. Fragments were then labeled and identified using GeneMapper software Version 4.0 (Applied Biosystems). Authenticity was confirmed against the ATCC STR profiling database (www.atcc.org/en/STR_Database.aspx) and the NCI-60 published data (17).

Cell viability assay. Cells were seeded in 96-well plates at a density of 2,000 (OVCAR3 and OV90) or 1,000 (OVCAR8) cells per well, and treated with ABT-263 and BMN 673 for the indicated time. Cell viability was determined using the XTT Cell Proliferation Assay kit (Trevigen, Gaithersburg, MD, USA) by comparing absorbance from the drug-treated cells with that from untreated cells at the same incubation period, unless otherwise specified. Absorbance at 450 nm with a reference wavelength of 650 nm was measured by the SpectraMax M5 reader (Molecular Devices, Sunnyvale, CA, USA). Each drug concentration was examined in duplicate or triplicate, and four independent experiments were performed. The IC_{50} values of ABT-263 and BMN 673 were calculated from concentration-effect curves by applying a four-parameter non-linear regression model using GraphPad Prism 7.0b software (GraphPad Software Inc., La Jolla, CA, USA).

Drug combination analysis. Combination synergism was analyzed by two different methods: the Chou-Talalay method using CompuSyn software (ComboSyn Inc., Paramus, NJ, USA) (18) and the Prichard-Shipman method using MacSynergy II software (Prichard and Shipman, University of Michigan, Ann Arbor, MI, USA) (19). The resulting combination index (CI) values define synergism (<0.9), additive (0.9-1.1), and antagonism (>1.1) in drug combinations (18). Synergy/antagonism volumes were statistically evaluated at the 95% confidence level and were expressed in $\mu M^2\%$, which are used to categorize the drug interactions: synergy (>25), additive (-25 to 25), and antagonism (<-25) (20).

Confocal immunofluorescence microscopy of γ-H2AX foci. Cells were seeded onto 12 mm poly L-lysine-coated coverslips (Corning Inc., Oneonta, NY, USA) in 24-well plates, and treated with 2 μM ABT-263 and 25 nM BMN 673 individually and in combination for 24 and 48 h. DMSO (0.002%) treatment was used as a vehicle control for this γ-H2AX immunofluorescence staining and all the experiments described below. Cells were washed in Dulbecco's PBS without calcium and magnesium upon completion of incubation, then fixed in 4% paraformaldehyde in PBS for 10 min. Permeabilization was performed with 0.25% Triton X-100 in PBS for 10 min, followed by blocking in 1% BSA in PBS for 1 h. Immunostaining was performed using the anti-γ-H2AX antibody (ab22551, 1:400 dilution, Abcam, Cambridge, MA, USA) for 1 h. Cells were washed three times with PBS, then incubated with the secondary antibody conjugated to Alexa Fluor 647 (A-21235, 1:200 dilution, Thermo Fisher Scientific Inc., Grand Island, NY, USA) for 1 h in the dark. Coverslips were mounted using Vectashield HardSet Antifade Mounting Medium with DAPI (Vector Laboratories, Burlingame, CA, USA), and slides were sealed and stored at 4˚C until imaging. The experiment was repeated at least four times on independent occasions per cell line at each time point for this γ-H2AX staining and all the experiments described below, unless otherwise specified. Confocal immunofluorescence microscopy imaging was performed using the LSM 780 laser-scanning confocal microscope (Carl Zeiss, Thornwood, NY, USA) with a 63x/1.4 oil immersion objective. A minimum of 120 cells were imaged per sample. Images were analyzed by counting the number of γ-H2AX foci using Focinator software (21), and noise tolerance level was set to 80. Cells with >5 foci in the nucleus were considered to be γ-H2AX foci-positive.

Cell cycle analysis. Cell cycle analysis was conducted using the APC BrdU Flow kit (BD Biosciences, San Jose, CA, USA). Cells were treated as described for the γ-H2AX immunofluorescence staining, then labeled with 10 μM BrdU for 1 h at 37˚C. Both floating and attached cells were harvested and subjected to the flow cytometric analysis according to the manufacturer's instructions. Stained cells were acquired on

Table I. Cytotoxic effects of ABT-263 and BMN 673.

	ABT-263 IC_{50} (μM)				BMN 673 IC_{50} (nM)	
	24 h	48 h	72 h	96 h	<72 h	96 h
OVCAR3	ND	5.00 (1.28)	4.07 (0.87)	4.50 (0.71)	ND	4.66 (0.80)
OVCAR8	ND	7.04 (1.78)	5.46 (0.58)	5.42 (0.22)	ND	88.2 (26.5)
OV90	6.70 (1.66)	1.65 (0.39)	1.51 (0.30)	1.48 (0.24)	ND	ND

IC_{50} values were calculated from the data of Fig. 1 and presented as the mean (SD) of four independent experiments. ND indicates that IC_{50} values were not determined because its cytotoxic effect was <50% even at the highest concentrations tested (8 μM and 100 nM for ABT-263 and BMN 673, respectively).

the FACSCalibur flow cytometer operated by CellQuest Pro software (BD Biosciences), and 25,000 events were collected per sample. The cell cycle distribution was analyzed using Flowjo 10.0.8r1 software (Tree Star Inc., Ashland, OR, USA).

Annexin V binding assay. Cells were treated as above, then both floating and attached cells were stained using the APC Annexin V Apoptosis Detection kit with 7-AAD (Biolegend, San Diego, CA, USA). Stained cells were measured using the FACSCalibur flow cytometer, and 25,000 events were collected per sample. The proportion of Annexin V-positive cells were gated and calculated using Flowjo 10.0.8r1 software.

Caspase activity assay. Caspase activity was determined using the Caspase-Glo 3/7 Assay kit (Promega, Madison, WI, USA). Cells were treated as above, and both floating and attached cells were harvested, pelleted, and subjected to the caspase activity assay. Briefly, cell pellets were lysed in modified RIPA buffer (50 mM Tris-HCl, pH 7.5, 150 mM NaCl, 10 μg/ml aprotinin, 1 mM phenylmethylsulfonyl fluoride, 10 μg/ml leupeptin, 2 mM Na_3VO_4, 4 mM EDTA, 10 mM NaF, 10 mM sodium pyrophosphate, 1% Nonidet P-40, and 0.1% sodium deoxycholate), supplemented with cOmplete Mini protease inhibitor cocktail tablets and PhosSTOP phosphatase inhibitor cocktail tablets (Roche Diagnostics, Indianapolis, IN, USA) and centrifuged at 14,000 rpm for 20 min. Protein concentration was determined using the Pierce BCA Protein Assay kit (Thermo Fisher Scientific Inc.). Ten micrograms of protein in a 50 μl total volume was mixed with 50 μl of equilibrated Caspase-Glo 3/7 reagent. After 30 min of incubation in the dark, luminescence was measured with the SpectraMax M5 reader.

Western blot analysis. Whole cell lysates were prepared as described for the caspase activity assay, and assessed by immunoblotting. Briefly, equal amounts of protein between 12.8 and 32.0 μg were separated by SDS-PAGE under reducing conditions on 14 or 16% Novex Tris-Glycine gels (Thermo Fisher Scientific Inc.) and electrophoretically transferred to 0.45 μm polyvinylidene difluoride membranes (EMD Millipore, Billerica, MA, USA). The XCell SureLock Mini-Cell and the XCell Blot Module (Thermo Fisher Scientific Inc.) were used for gel electrophoresis and protein transfer, according to the manufacturer's instructions. After incubation with 5% non-fat dry milk in TBS containing 0.1% Tween-20 (TBST) for 1 h, membranes were washed once with TBST and probed with the indicated primary antibodies overnight at 4˚C. The following primary antibodies were used: cleaved PARP (#5625), β-tubulin (#2128), Bcl-2 (#4223), Bcl-xL (#2764), Mcl-1 (#5453), Bax (#5023), Bak (#12105), Bim (#2933), Bid (#2002) (all from Cell Signaling Technology, Danvers, MA, USA), Puma (ab33906), and Noxa (ab13654) (both from Abcam). All the primary antibodies were diluted 1:1,000 in TBST containing 5% BSA, except β-tubulin and Bcl-xL, which were diluted 1:10,000. Membranes were washed three times with TBST and incubated with 1:5,000 dilution of horseradish peroxidase-conjugated anti-mouse or rabbit antibodies (Thermo Fisher Scientific Inc.) for 1 h. After washing three times with TBST, membranes were incubated with SuperSignal West Pico or Dura Chemiluminescent Substrate (Thermo Fisher Scientific Inc.) for 5 min. Chemiluminescent signals were visualized by exposing the membrane to X-ray film (HyBlot ES Autoradiography Film, Denville Scientific Inc., Holliston, MA, USA). Immunoblot analyses were performed at least three times for all the antibodies. Densitometry was performed using ImageJ 1.50b software (NIH, Bethesda, MD, USA). Densitometry values were normalized to the loading control β-tubulin and expressed as relative fold changes compared to DMSO-treated cells.

Statistical analysis. For multiple comparisons, the results were analyzed by a two-way ANOVA and the Dunnett post hoc test to compare the mean of each group with the combination treatment group using GraphPad Prism 7.0b software. All differences were considered statistically significant at $p<0.05$.

Results

Sensitivity of HGSOC cells to single agent treatment. Effects of ABT-263 (0.125-8 μM) and BMN 673 (1.56-100 nM) monotherapy on cell viability of three HGSOC cell lines were evaluated at 24, 48, 72, and 96 h after initiation of drug treatment. The concentration-effect curves are shown in Fig. 1. Both ABT-263 and BMN 673 caused a concentration-dependent growth inhibition in all cell lines. The effect of BMN 673 was deemed more treatment time-dependent than that of ABT-263 in each cell line. BMN 673 treatment achieved modest cell growth inhibition during the first 48 h, followed by significant growth inhibition during the last 48 h. By contrast, ABT-263 treatment resulted in maximum cytotoxic effects within 48 h, and almost no change in IC_{50} values after 48 h (Table I).

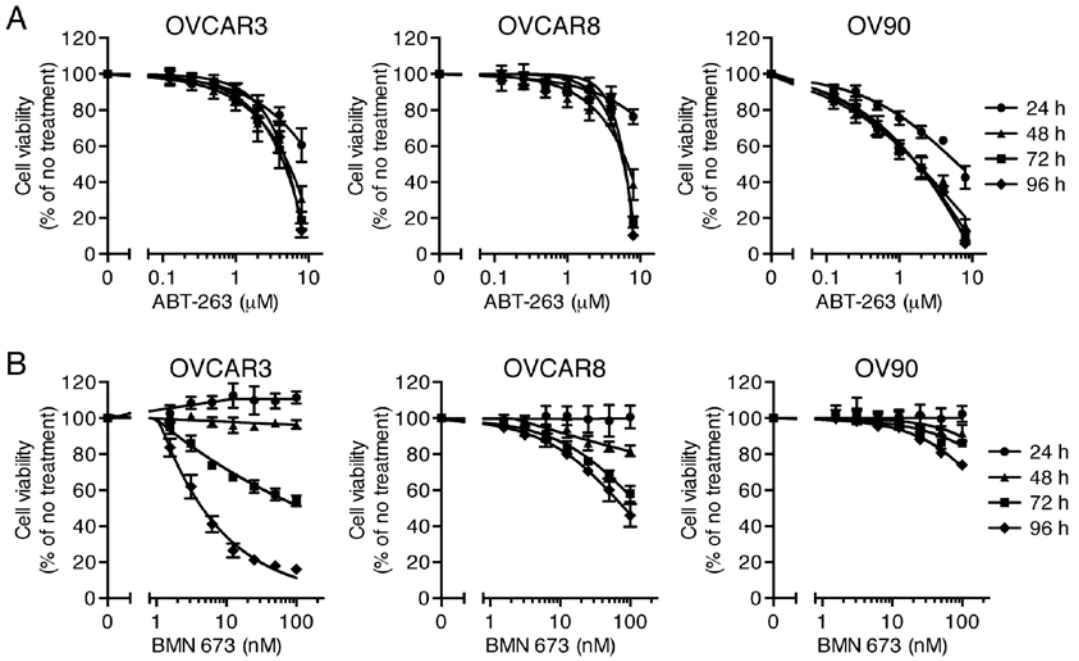

Figure 1. Effects of single agent treatment on cell viability. Three HGSOC cell lines were treated with ABT-263 (A) or BMN 673 (B) for 24-96 h. The percentage of cell viability relative to untreated cells was determined using the XTT assay and shown as the mean ± SD of four independent experiments performed in duplicate.

Table II. Combination index (CI) values and synergy/antagonism volumes after 72 h of treatment.

	CI values at inhibition of			
	50%	75%	90%	Synergy/antagonism volumes (μM^2%)
OVCAR3	0.52 (0.05)	0.58 (0.09)	0.71 (0.13)	150/-5
OVCAR8	0.34 (0.02)	0.29 (0.06)	0.29 (0.11)	345/0
OV90	0.57 (0.11)	0.58 (0.25)	0.89 (0.60)	225/0

CI values and synergy/antagonism volumes were calculated from the data of Fig. 2A using CompuSyn software and MacSynergy II software, respectively. CI values are presented as the mean (SD) of four independent experiments, and values <0.9 indicate synergy. Synergy/antagonism volumes were calculated at the 95% confidence level from four independent experiments, and volumes >25 indicate synergy.

The combination of ABT-263 and BMN 673 synergistically inhibits HGSOC cell proliferation. To examine the cytotoxic effects of the combination treatment, three HGSOC cell lines were treated with indicated concentrations of ABT-263 alone and in combination with BMN 673 for 72 h (and 24-96 h for time course experiments). All the concentration-effect curves for the combination treatment showed an apparent leftward shift compared to the monotherapy curve in each cell line (Fig. 2A), indicating synergy (22). Table II shows the CI values and synergy/antagonism volumes for each cell line with the combination treatment for 72 h. Synergistic cytotoxicity was confirmed across all cell lines with the CI values at 50, 75, and 90% inhibition all <0.9 (18), and the synergy/antagonism volumes at 95% confidence all >100 (20). Time course of cell viability was measured as a function of the XTT assay absolute absorbance value. The combination treatment completely inhibited growth of OVCAR3 and OVCAR8 cells when each monotherapy showed a modest effect (Fig. 2B).

DNA fragmentation is significantly increased by the combination treatment. PARPi cause DNA damage accumulation and G2/M cell cycle arrest (23,24). Effects of ABT-263 and BMN 673 on DNA double-strand break induction and cell cycle progression were thus examined to dissect the potential mechanisms of cell growth inhibition induced by the combination treatment. BMN 673 monotherapy induced γ-H2AX foci formation in all cell lines as early as 24 h after treatment (Fig. 3). ABT-263 alone or in combination with BMN 673 did not significantly induce γ-H2AX foci formation compared with the control or BMN 673 monotherapy, respectively. The cell cycle analysis indicated that BMN 673 treatment induced G2/M phase accumulation in all cell lines as early as 24 h after treatment, in the presence or absence of ABT-263 (Figs. 4 and 5A). ABT-263 monotherapy did not significantly change the cell cycle distribution compared with the control. Notably, the combination treatment induced sub-G1 phase accumulation compared with the control and each monotherapy after

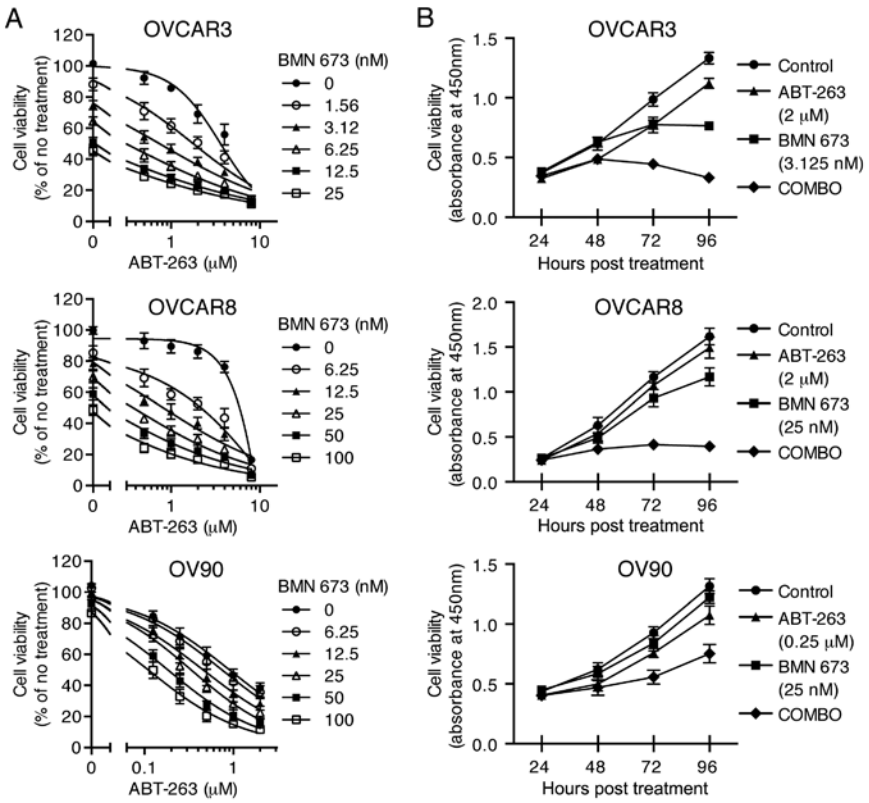

Figure 2. Combination treatment synergistically decreased cell viability. The combined treatment with ABT-263 and BMN 673 against three HGSOC cell lines was evaluated in a concentration- (A, 72 h) or time-dependent (B, 24-96 h) manner. The percentage of cell viability relative to untreated cells (A) and the absolute absorbance value (B) were determined using the XTT assay and shown as the mean ± SD of four independent experiments performed in triplicate (A) or duplicate (B).

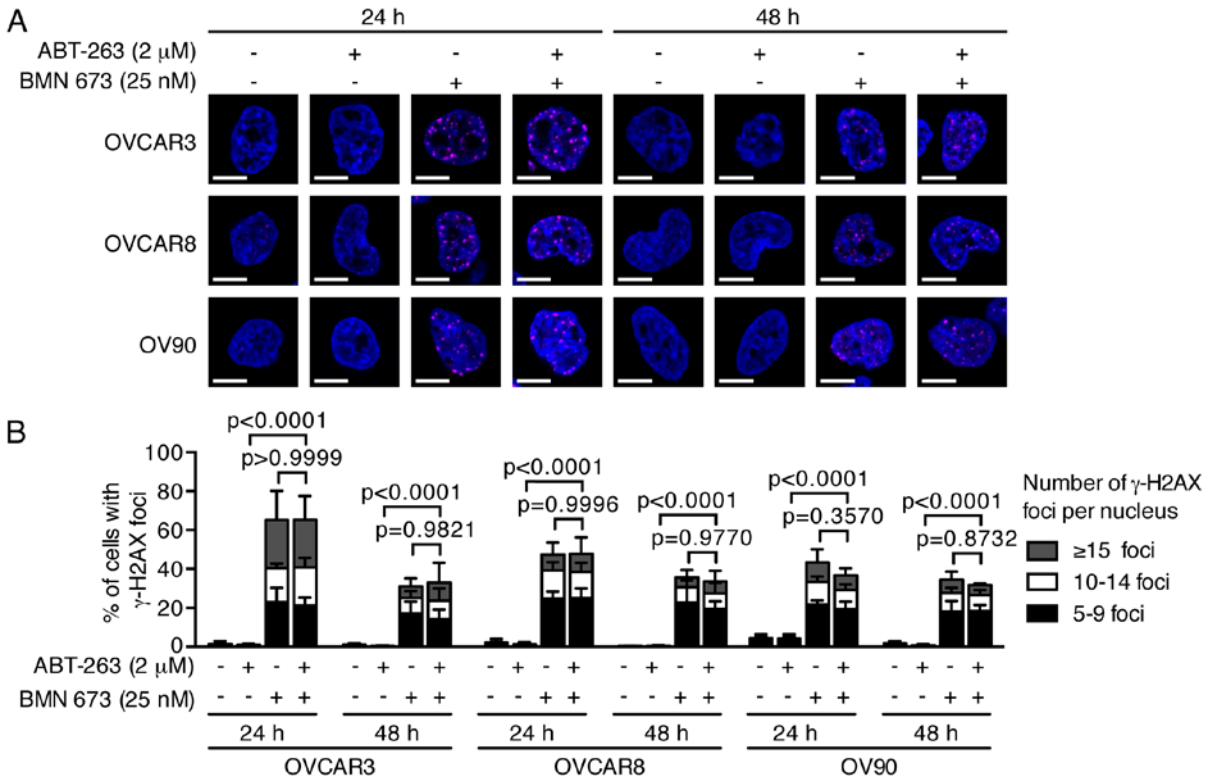

Figure 3. Treatment effects on DNA damage. Three HGSOC cell lines were treated as described then assessed by staining for γ-H2AX and confocal immunofluorescence imaging. DMSO (0.002%) treatment was used as a vehicle control. (A) Representative images of at least four independent experiments are shown. γ-H2AX foci are colored in magenta, and nuclei are colored blue. Scale bar, 10 μm. (B) The percentage of γ-H2AX foci-positive cells (>5 γ-H2AX foci in nucleus) was determined by analyzing >120 cells per condition and shown as the mean ± SD of at least four independent experiments. P-values were calculated by a two-way ANOVA.

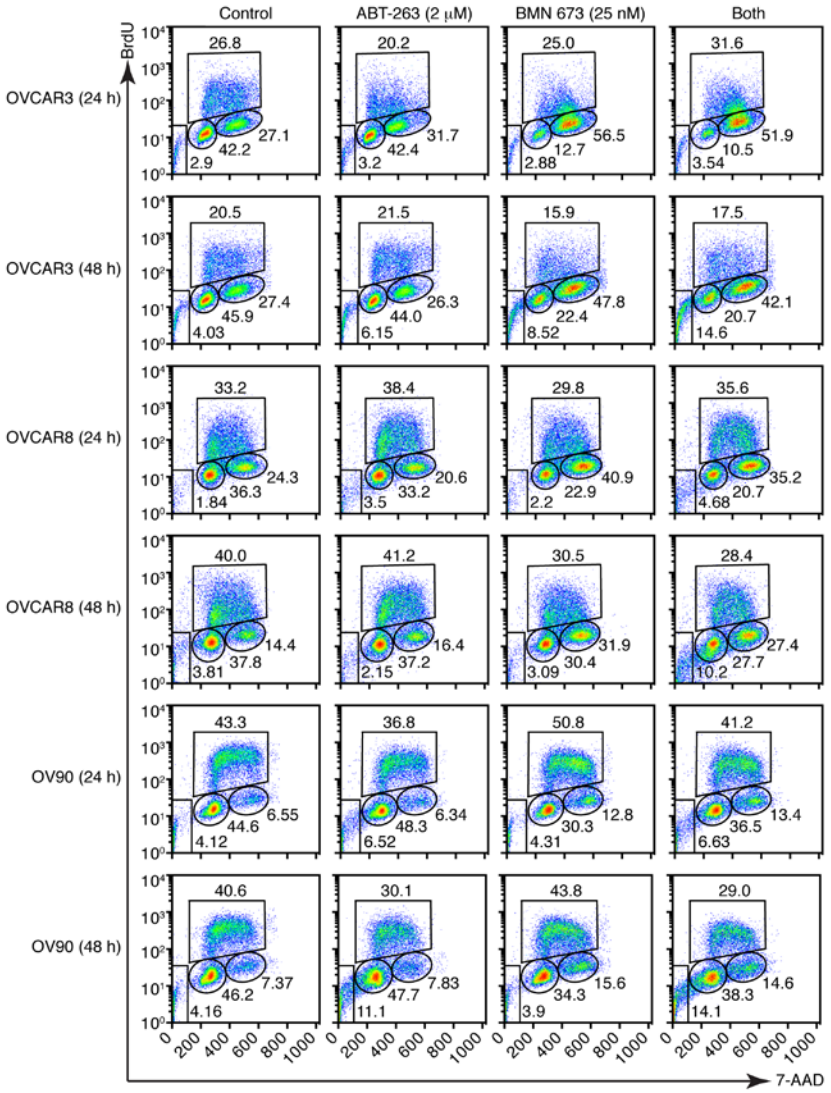

Figure 4. Treatment effects on cell cycle distribution. Three HGSOC cell lines were treated as described then assessed by flow cytometric measurement of DNA content. DMSO (0.002%) treatment was used as a vehicle control. Representative pseudocolor dot plots of four independent experiments are shown.

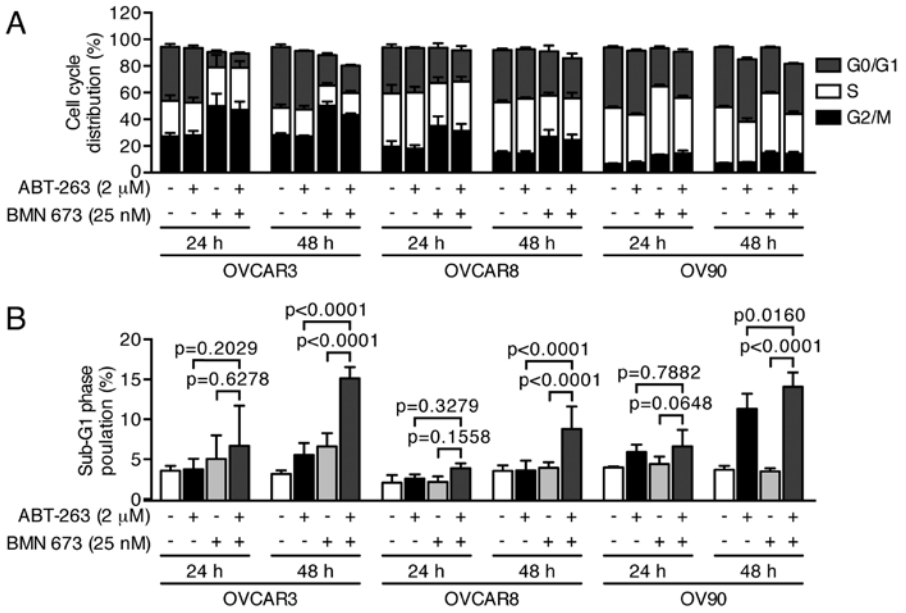

Figure 5. Combination treatment significantly increased DNA fragmentation. Three HGSOC cell lines were treated as described then assessed by flow cytometric measurement of DNA content. DMSO (0.002%) treatment was used as a vehicle control. The percentages of cells in each cell cycle phase (A) and the sub-G1 phase (B) are shown as the mean ± SD of four independent experiments. P-values were calculated by a two-way ANOVA.

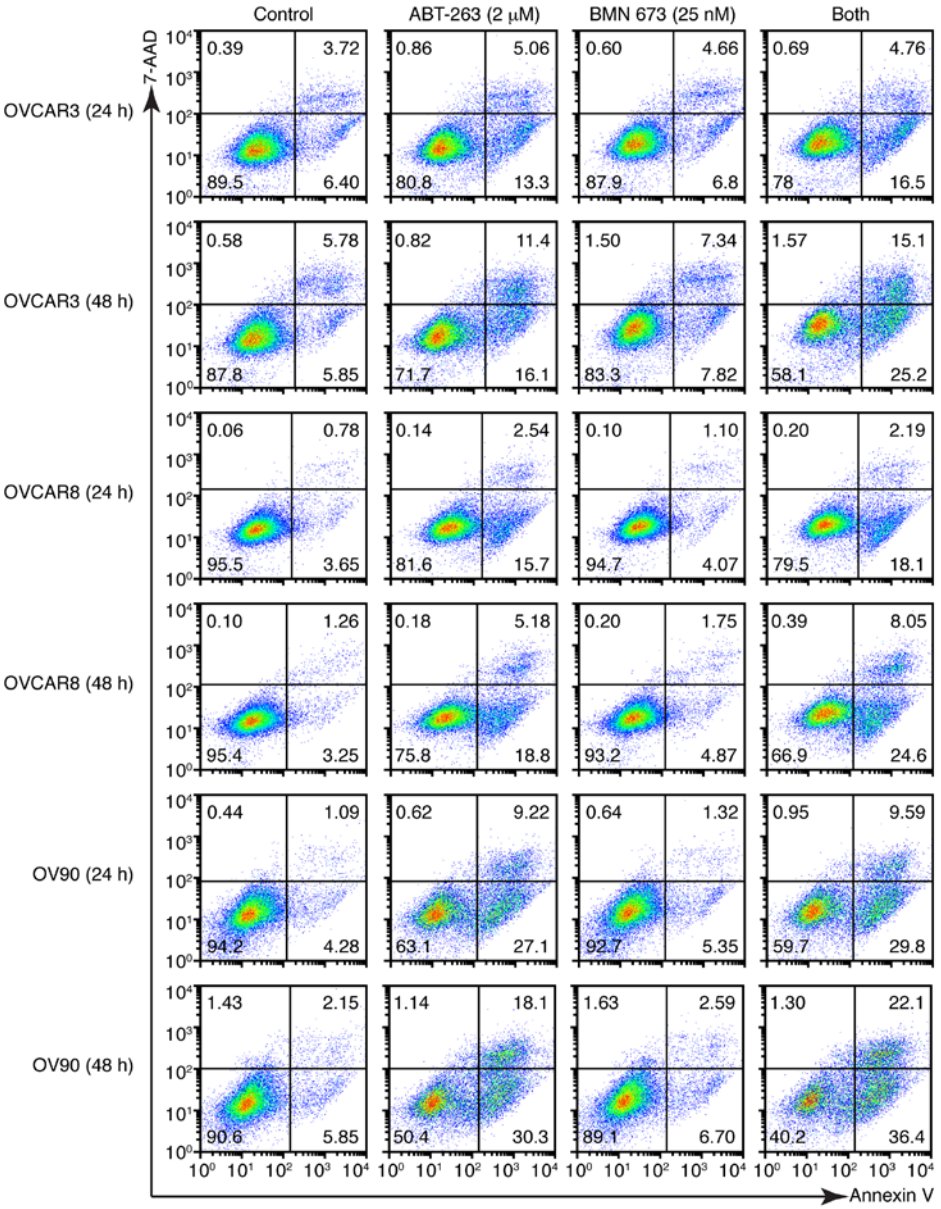

Figure 6. Combination treatment increased Annexin V-positive cells. Three HGSOC cell lines were treated as described followed by analysis using the Annexin V binding assay. DMSO (0.002%) treatment was used as a vehicle control. Representative pseudocolor dot plots of four independent experiments are shown.

48 h of treatment, indicating an increase in DNA fragmentation (Figs. 4 and 5B).

Combination treatment significantly induces apoptotic cell death via a caspase-dependent pathway. We next examined whether growth inhibition and DNA fragmentation induced by the combination treatment were attributable to apoptotic cell death. The combination treatment induced a higher percentage of Annexin V-positive cells compared with the control and each monotherapy in all cell lines after 48 h (Figs. 6 and 7A). We evaluated the caspase-3/7 activity and PARP cleavage to further verify the apoptotic nature of cell death induced by the combination treatment. Fig. 7B shows a significant increase of caspase-3/7 activity after 48 h of the combination treatment compared with the control and each monotherapy in all cell lines. This was accompanied by an increased cleaved PARP expression after 48 h of the combination treatment, suggesting that a caspase-dependent apoptotic pathway was activated in response to the combination treatment (Fig. 7C).

ABT-263 alone and in combination with BMN 673 induces expression levels of Mcl-1, Bim, and Noxa. We evaluated possible alterations in the expression levels of pro- and anti-apoptotic Bcl-2 family proteins to further explore molecular mechanisms of increased apoptosis by the combination treatment (Fig. 8). BMN 673 monotherapy had little effect on most proteins examined after 48 h of treatment. ABT-263 monotherapy and the combination treatment increased Mcl-1, Bim, and Noxa protein expression. Notably, Bid expression was decreased by the combination treatment, but not by either monotherapy.

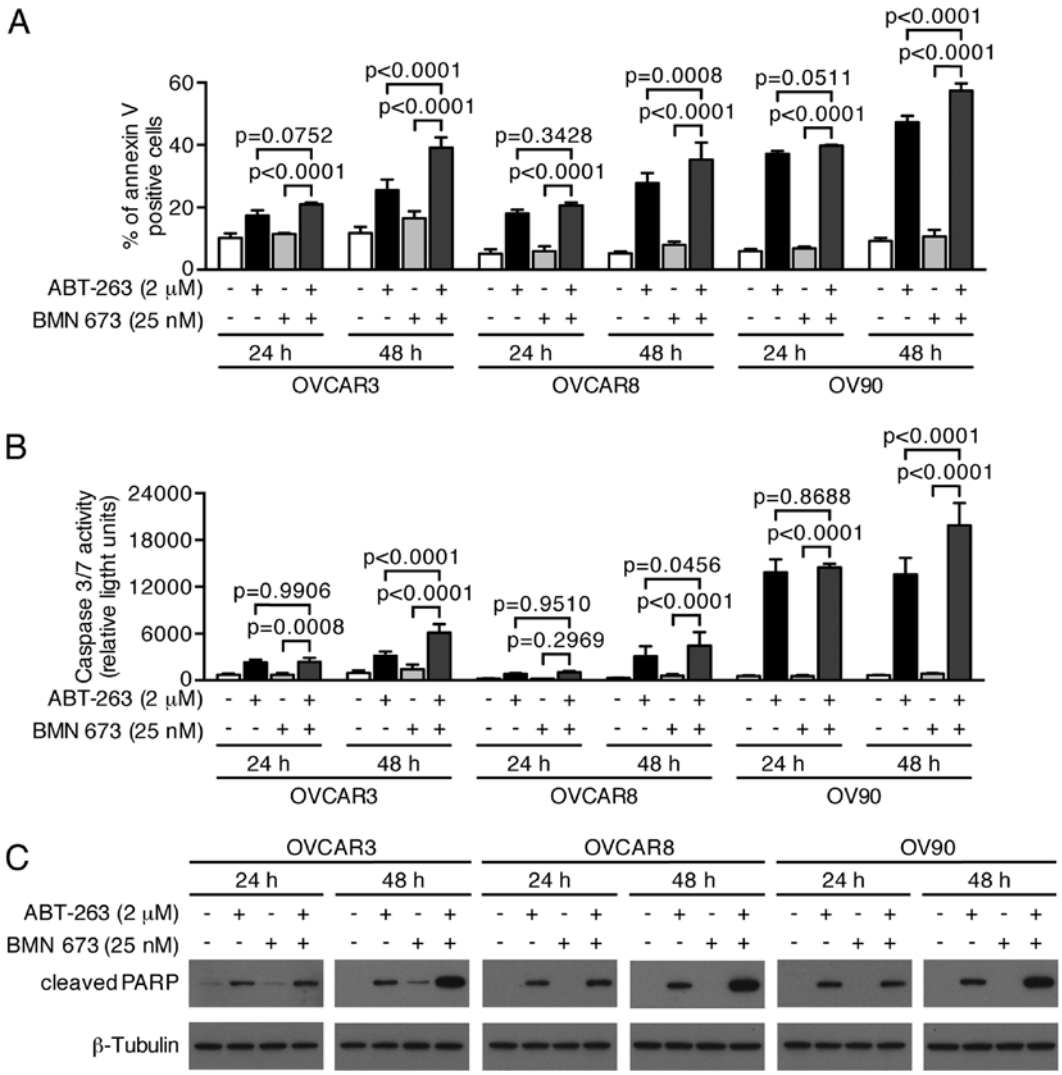

Figure 7. Combination treatment significantly increased apoptotic cell death. Three HGSOC cell lines were treated as described followed by analysis using the Annexin V binding assay (A), the caspase activity assay (B), and immunoblotting (C). DMSO (0.002%) treatment was used as a vehicle control. (A) The percentages of Annexin V-positive cells are shown as the mean ± SD of four independent experiments. P-values were calculated by a two-way ANOVA. (B) Graph shows the mean ± SD of four independent experiments performed in duplicate. P-values were calculated by a two-way ANOVA. (C) Whole cell lysates were subjected to immunoblotting. Images are representative of three independent experiments.

Discussion

Modulation of apoptotic pathways is a promising therapeutic strategy in HGSOC. Here, we report a novel benefit of the combination treatment with ABT-263 and BMN 673 against HGSOC cells. The combination treatment showed synergistic cytotoxic effects based on two different methods: the Chou-Talalay method (18) and the Prichard-Shipman method (19). Synergistic cytotoxicity was further investigated by several assays, including the Annexin V binding assay, the caspase-3/7 activity assay, and cleaved PARP detection by immunoblotting. We observed significantly increased apoptosis following the combination treatment compared with either monotherapy.

The drug concentrations used in this study were carefully selected to perform a clinically relevant *in vitro* study (25). Synergistic cytotoxic effects were induced by the combination treatment at clinically achievable concentrations, which are below the peak plasma concentrations of recommended phase 2 doses for each drug (5.33-6.61 μM and 50 nM for ABT-263 and BMN 673, respectively) (15,26,27).

We examined the drug effects on DNA damage and cell cycle distribution to explore the potential mechanisms of the observed synergistic cytotoxic effects. BMN 673 treatment induced accumulation of γ-H2AX foci and the proportional increase of cells in the G2/M phase, as previously reported (28). ABT-263 monotherapy did not induce γ-H2AX foci formation or affect the cell cycle distribution, consistent with previous reports (29,30). The addition of ABT-263 did not affect either γ-H2AX foci formation or G2/M cell cycle arrest induced by BMN 673 treatment, suggesting the observed synergistic cytotoxicity was unlikely due to augmented DNA damage accumulation.

Several chemotherapeutic agents have shown synergy with ABT-263 based on two main mechanisms, either decreased expression of Mcl-1 or increased expression of BH3-only proteins (31). BMN 673 treatment neither decreased the expression of Mcl-1 nor increased the expression of BH3-only proteins.

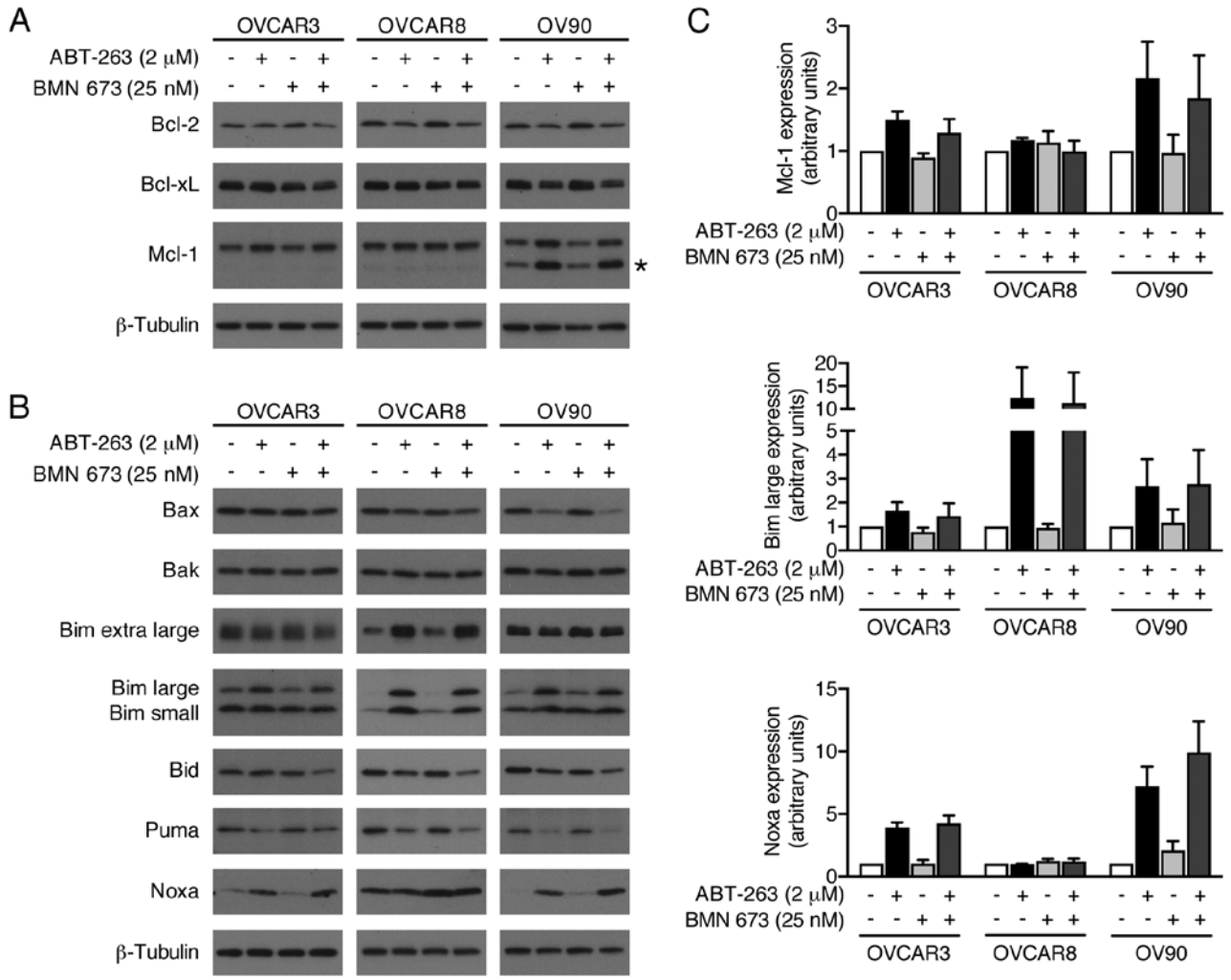

Figure 8. Effects of ABT-263 and BMN 673 on expression levels of Bcl-2 family proteins. Whole cell lysates were prepared from three HGSOC cell lines treated as described for 48 h, and the expression of Bcl-2 family proteins was detected by immunoblotting. DMSO (0.002%) treatment was used as a vehicle control. Representative images of anti-apoptotic proteins (A) and pro-apoptotic proteins (B) are shown from at least three independent experiments. The asterisk indicates non-specific bands. (C) Quantitative analysis of immunoblotting. Graph shows the mean ± SD of fold change in protein expression relative to DMSO-treated cells (n=3). β-tubulin was used as the loading control for normalization.

Our findings confirmed ABT-263 treatment increased Mcl-1, Bim, and Noxa expression, as shown previously (32-34). It has been reported that ABT-263 posttranscriptionally upregulates Mcl-1 expression through ERK-mediated phosphorylation of Mcl-1 on Thr-163 (33,34). Mcl-1 confers resistance to ABT-263 because it remains a potent anti-apoptotic protein (31). However, expression of Mcl-1 is not always sufficient to cause resistance to ABT-263 given that occupancy of Mcl-1 by pro-apoptotic proteins can effectively inactivate Mcl-1 (15,35,36). The extent of pro-apoptotic Bcl-2 family proteins occupancy by anti-apoptotic proteins correlates well with the observed clinical response to chemotherapy, and could be modulated to enhance chemosensitivity (37). Thus, we speculated that ABT-263 treatment did not necessarily enhance the effects of BMN 673 treatment, but might have lowered the apoptotic threshold by increasing Bim and Noxa pro-apoptotic protein expression, leading to greater susceptibility to addition of BMN 673 treatment (38). During apoptosis, Bid can be cleaved and activated by caspase-3 as well as caspase-8 (39). Although we did not observe the occurrence of cleaved Bid, we found that the expression of full length Bid was decreased by the combination treatment, but not by either monotherapy, implying increased caspase activity by the combination treatment.

ABT-263 monotherapy is currently under clinical investigation in women with platinum resistant/refractory recurrent ovarian cancer (NCT02591095). Platelet survival is dependent on Bcl-xL and, as would be expected, clinically significant and sometimes dose-limiting thrombocytopenia has been observed with ABT-263 treatment (15,26). PARPi, as a class, also result in hematotoxicity, including reduction in platelets with rare significant thrombocytopenia, although this class of agents has been documented to have activity at submaximal doses when used in combination treatments (40,41). Synergistic drug combinations carry the expectation of greater therapeutic efficacy, although they may also increase the severity of adverse effects. Careful dose escalation and close monitoring would be needed for further clinical investigation.

In conclusion, combined treatment with ABT-263 and BMN 673 synergistically inhibited HGSOC cell proliferation at clinically achievable concentrations. The combination

treatment significantly increased apoptotic cell death through caspase activation compared with either monotherapy. A pro-apoptotic environment augmented by ABT-263 might be a possible mechanism of the observed synergistic cytotoxic effects. Our results support further evaluation of the therapeutic potential of the combination treatment including BH3-mimetics and PARPi for HGSOC.

Acknowledgements

The authors would like to thank the Center for Cancer Research Confocal Microscopy Core Facility (NCI/NIH, Bethesda, MD, USA) for technical assistance. This study was supported by the Intramural Program of the Center for Cancer Research, National Cancer Institute, National Institutes of Health.

References

1. Siegel RL, Miller KD and Jemal A: Cancer statistics, 2016. CA Cancer J Clin 66: 7-30, 2016.
2. Coleman RL, Monk BJ, Sood AK and Herzog TJ: Latest research and treatment of advanced-stage epithelial ovarian cancer. Nat Rev Clin Oncol 10: 211-224, 2013.
3. Bowtell DD, Böhm S, Ahmed AA, Aspuria PJ, Bast RC Jr, Beral V, Berek JS, Birrer MJ, Blagden S, Bookman MA, *et al*: Rethinking ovarian cancer II: Reducing mortality from high-grade serous ovarian cancer. Nat Rev Cancer 15: 668-679, 2015.
4. Bell D, Berchuck A, Birrer M, Chien J, Cramer DW, Dao F, Dhir R, DiSaia P, Gabra H, Glenn P, *et al*; Cancer Genome Atlas Research Network: Integrated genomic analyses of ovarian carcinoma. Nature 474: 609-615, 2011.
5. Gelmon KA, Tischkowitz M, Mackay H, Swenerton K, Robidoux A, Tonkin K, Hirte H, Huntsman D, Clemons M, Gilks B, *et al*: Olaparib in patients with recurrent high-grade serous or poorly differentiated ovarian carcinoma or triple-negative breast cancer: A phase 2, multicentre, open-label, non-randomised study. Lancet Oncol 12: 852-861, 2011.
6. Kim G, Ison G, McKee AE, Zhang H, Tang S, Gwise T, Sridhara R, Lee E, Tzou A, Philip R, *et al*: FDA Approval Summary: Olaparib monotherapy in patients with deleterious germline BRCA-mutated advanced ovarian cancer treated with three or more lines of chemotherapy. Clin Cancer Res 21: 4257-4261, 2015.
7. Parkes EE and Kennedy RD: Clinical application of poly(ADP-ribose) polymerase inhibitors in high-grade serous ovarian cancer. Oncologist 21: 586-593, 2016.
8. Murai J, Huang SY, Renaud A, Zhang Y, Ji J, Takeda S, Morris J, Teicher B, Doroshow JH and Pommier Y: Stereospecific PARP trapping by BMN 673 and comparison with olaparib and rucaparib. Mol Cancer Ther 13: 433-443, 2014.
9. Aredia F and Scovassi AI: Poly(ADP-ribose): A signaling molecule in different paradigms of cell death. Biochem Pharmacol 92: 157-163, 2014.
10. Delbridge AR, Grabow S, Strasser A and Vaux DL: Thirty years of BCL-2: Translating cell death discoveries into novel cancer therapies. Nat Rev Cancer 16: 99-109, 2016.
11. Williams J, Lucas PC, Griffith KA, Choi M, Fogoros S, Hu YY and Liu JR: Expression of Bcl-xL in ovarian carcinoma is associated with chemoresistance and recurrent disease. Gynecol Oncol 96: 287-295, 2005.
12. Wong M, Tan N, Zha J, Peale FV, Yue P, Fairbrother WJ and Belmont LD: Navitoclax (ABT-263) reduces Bcl-x(L)-mediated chemoresistance in ovarian cancer models. Mol Cancer Ther 11: 1026-1035, 2012.
13. Witham J, Valenti MR, De-Haven-Brandon AK, Vidot S, Eccles SA, Kaye SB and Richardson A: The Bcl-2/Bcl-XL family inhibitor ABT-737 sensitizes ovarian cancer cells to carboplatin. Clin Cancer Res 13: 7191-7198, 2007.
14. Rudin CM, Hann CL, Garon EB, Ribeiro de Oliveira M, Bonomi PD, Camidge DR, Chu Q, Giaccone G, Khaira D, Ramalingam SS, *et al*: Phase II study of single-agent navitoclax (ABT-263) and biomarker correlates in patients with relapsed small cell lung cancer. Clin Cancer Res 18: 3163-3169, 2012.
15. Roberts AW, Seymour JF, Brown JR, Wierda WG, Kipps TJ, Khaw SL, Carney DA, He SZ, Huang DC, Xiong H, *et al*: Substantial susceptibility of chronic lymphocytic leukemia to BCL2 inhibition: Results of a phase I study of navitoclax in patients with relapsed or refractory disease. J Clin Oncol 30: 488-496, 2012.
16. Domcke S, Sinha R, Levine DA, Sander C and Schultz N: Evaluating cell lines as tumour models by comparison of genomic profiles. Nat Commun 4: 2126, 2013.
17. Lorenzi PL, Reinhold WC, Varma S, Hutchinson AA, Pommier Y, Chanock SJ and Weinstein JN: DNA fingerprinting of the NCI-60 cell line panel. Mol Cancer Ther 8: 713-724, 2009.
18. Chou TC: Theoretical basis, experimental design, and computerized simulation of synergism and antagonism in drug combination studies. Pharmacol Rev 58: 621-681, 2006.
19. Prichard MN and Shipman C Jr: A three-dimensional model to analyze drug-drug interactions. Antiviral Res 14: 181-205, 1990.
20. Prichard MK, Aseltine KR and Shipman C Jr: MacSynergy II, ver sion 1.0. User's manual. University of Michigan, Ann Arbor, MI, 1993.
21. Oeck S, Malewicz nM, Hurst S, Rudner J and Jendrossek V: The Focinator - a new open-source tool for high-throughput foci evaluation of DNA damage. Radiat Oncol 10: 163, 2015.
22. Zhao L, Wientjes MG and Au JL-S: Evaluation of combination chemotherapy: Integration of nonlinear regression, curve shift, isobologram, and combination index analyses. Clin Cancer Res 10: 7994-8004, 2004.
23. Farmer H, McCabe N, Lord CJ, Tutt AN, Johnson DA, Richardson TB, Santarosa M, Dillon KJ, Hickson I, Knights C, *et al*: Targeting the DNA repair defect in BRCA mutant cells as a therapeutic strategy. Nature 434: 917-921, 2005.
24. Herriott A, Tudhope SJ, Junge G, Rodrigues N, Patterson MJ, Woodhouse L, Lunec J, Hunter JE, Mulligan EA, Cole M, *et al*: PARP1 expression, activity and ex vivo sensitivity to the PARP inhibitor, talazoparib (BMN 673), in chronic lymphocytic leukaemia. Oncotarget 6: 43978-43991, 2015.
25. Smith MA and Houghton P: A proposal regarding reporting of in vitro testing results. Clin Cancer Res 19: 2828-2833, 2013.
26. Wilson WH, O'Connor OA, Czuczman MS, LaCasce AS, Gerecitano JF, Leonard JP, Tulpule A, Dunleavy K, Xiong H, Chiu YL, *et al*: Navitoclax, a targeted high-affinity inhibitor of BCL-2, in lymphoid malignancies: A phase 1 dose-escalation study of safety, pharmacokinetics, pharmacodynamics, and antitumour activity. Lancet Oncol 11: 1149-1159, 2010.
27. De Bono JSML, Gonzalez M, Curtin NJ, Wang E, Henshaw JW, Chadha M, Sachdev JC, Matei D, Jameson GS, Ong M, *et al*: First-in-human trial of novel oral PARP inhibitor BMN 673 in patients with solid tumors. J Clin Oncol 31: 2580, 2013.
28. Shen Y, Rehman FL, Feng Y, Boshuizen J, Bajrami I, Elliott R, Wang B, Lord CJ, Post LE and Ashworth A: BMN 673, a novel and highly potent PARP1/2 inhibitor for the treatment of human cancers with DNA repair deficiency. Clin Cancer Res 19: 5003-5015, 2013.
29. Tan N, Wong M, Nannini MA, Hong R, Lee LB, Price S, Williams K, Savy PP, Yue P, Sampath D, *et al*: Bcl-2/Bcl-xL inhibition increases the efficacy of MEK inhibition alone and in combination with PI3 kinase inhibition in lung and pancreatic tumor models. Mol Cancer Ther 12: 853-864, 2013.
30. Green MM, Shekhar TM and Hawkins CJ: Data on the DNA damaging and mutagenic potential of the BH3-mimetics ABT-263/Navitoclax and TW-37. Data Brief 6: 710-714, 2016.
31. Stamelos VA, Redman CW and Richardson A: Understanding sensitivity to BH3 mimetics: ABT-737 as a case study to foresee the complexities of personalized medicine. J Mol Signal 7: 12, 2012.
32. Wang H, Yang YB, Shen HM, Gu J, Li T and Li XM: ABT-737 induces Bim expression via JNK signaling pathway and its effect on the radiation sensitivity of HeLa cells. PLoS One 7: e52483, 2012.
33. Wang B, Ni Z, Dai X, Qin L, Li X, Xu L, Lian J and He F: The Bcl-2/xL inhibitor ABT-263 increases the stability of Mcl-1 mRNA and protein in hepatocellular carcinoma cells. Mol Cancer 13: 98, 2014.
34. Hiraki M, Suzuki Y, Alam M, Hinohara K, Hasegawa M, Jin C, Kharbanda S and Kufe D: MUC1-C stabilizes MCL-1 in the oxidative stress response of triple-negative breast cancer cells to BCL-2 inhibitors. Sci Rep 6: 26643, 2016.
35. Morales AA, Kurtoglu M, Matulis SM, Liu J, Siefker D, Gutman DM, Kaufman JL, Lee KP, Lonial S and Boise LH: Distribution of Bim determines Mcl-1 dependence or codependence with Bcl-xL/Bcl-2 in Mcl-1-expressing myeloma cells. Blood 118: 1329-1339, 2011.

36. Yamaguchi R, Janssen E, Perkins G, Ellisman M, Kitada S and Reed JC: Efficient elimination of cancer cells by deoxyglucose-ABT-263/737 combination therapy. PLoS One 6: e24102, 2011.
37. Ni Chonghaile T, Sarosiek KA, Vo TT, Ryan JA, Tammareddi A, Moore VG, Deng J, Anderson KC, Richardson P, Tai YT, *et al*: Pretreatment mitochondrial priming correlates with clinical response to cytotoxic chemotherapy. Science 334: 1129-1133, 2011.
38. Lopez J and Tait SW: Mitochondrial apoptosis: Killing cancer using the enemy within. Br J Cancer 112: 957-962, 2015.
39. Slee EA, Keogh SA and Martin SJ: Cleavage of BID during cytotoxic drug and UV radiation-induced apoptosis occurs downstream of the point of Bcl-2 action and is catalysed by caspase-3: A potential feedback loop for amplification of apoptosis-associated mitochondrial cytochrome c release. Cell Death Differ 7: 556-565, 2000.
40. Lee JM, Hays JL, Annunziata CM, Noonan AM, Minasian L, Zujewski JA, Yu M, Gordon N, Ji J, Sissung TM, *et al*: Phase I Ib study of olaparib and carboplatin in BRCA1 or BRCA2 mutation-associated breast or ovarian cancer with biomarker analyses. J Natl Cancer Inst 106: dju089, 2014.
41. Oza AM, Cibula D, Benzaquen AO, Poole C, Mathijssen RH, Sonke GS, Colombo N, Špaček J, Vuylsteke P, Hirte H, *et al*: Olaparib combined with chemotherapy for recurrent platinum-sensitive ovarian cancer: A randomised phase 2 trial. Lancet Oncol 16: 87-97, 2015.